Soft Adsorption of Densely Packed Layers of DNA- Plasmid • 1,3-diaminopropane Complexes onto Highly Oriented Pyrolitic Graphite designed to Erode in Water

Omar Boulanouar, [†] ***Abderrahim Khatyr,*** [‡] ***Guillaume Herlem,*** [‡] ***Frank Palmino,*** [♠] ***Léon Sanche*** [§] ***and Michel Fromm*** [*†]

[†] Laboratoire de Chimie-Physique et Rayonnements - Alain Chambaudet (LCPR-AC), UMR CEA E4. Université de Franche-Comté. 16 Route de Gray. F-25030 Besançon Cedex,

[‡] Institut UTINAM, UMR CNRS 6213. Université de Franche-Comté. 16 Route de Gray. F-25030 BESANCON Cedex

[♠] Institut FEMTO-ST, Université de Franche-Comté, CNRS, ENSMM, 32, Avenue de l'Observatoire, 25044 Besancon cedex (France)

[§] Groupe de Recherche en Sciences des Radiations, Faculté de Médecine et des Sciences de la Santé, Université de Sherbrooke, Sherbrooke, Québec J1H 5N4, Canada

Corresponding author: michel.fromm@univ-fcomte.fr

Tél.: (0) 33 3 81 66 65 60

Fax.: (0) 33 3 81 66 65 22

Abstract:

In this paper we report a simple and effective method to build up self-assembled and well-calibrated layers of plasmid DNA • 1,3-diaminopropane complexes onto Highly Oriented Pyrolitic Graphite (HOPG). The method is based on the self-assembly of the poly-electrolytes onto HOPG in an excess of positively-charged protonated di-amines (Dap^{2+}) in comparison to the negatively-charged phosphate moieties of the DNA backbone in solution. Although short distortions in the helical parameters of DNA (maximum 12% hypochromicity) are revealed by UV-Vis absorption spectrometry, the native B form of the plasmids is conserved. By fixing the excess of positive charges arising from Dap^{2+} cations, it is possible to construct assemblies of a well-defined thickness ranging typically from 1 monolayer (ML) of DNA to 10 ML; 1 ML has a thickness of 2.2 ± 0.5 nm. Adding TRIS-EDTA (TE) buffer lowers considerably the damage rate observed when plasmids are mixed to Dap^{2+} in pure water. The thickness of the first dense mono-layer matches well the DNA cross-sectional dimensions indicating that this layer is strongly anchored to the surface; it is insoluble in water. Conversely, thicker layers can be released in aqueous media and the plasmids do not undergo dramatic damage. In presence of TE buffer condensation of the plasmids on the HOPG surface and a further release of the deposits in water yields a loss of supercoiling that ranges typically from 10 to 20% when the layer thickness varies from 22 to 12 nanometers. Such densely-packed and releasable DNA plasmid layers with a very well characterized and constant thickness constitute a substantial progress for biochemical and radiochemical experiments.

Introduction

The interest for DNA-based structures deposited onto surfaces has promoted a large variety of studies in the last decades. DNA macromolecular assemblies are needed in radiological experiments and for various applications such as biosensing or gene delivery,[1] self-assembly nanostructures[2,3] and production of 2D templates or scaffolds for the construction of nanomaterials. Fabrication of such structures usually requires well characterized single or double stranded oligonucleotides, which are physisorbed or chemically bonded to an atomically smooth surface. Under such well controlled conditions, the DNA-based structures can usually be characterized and visualized by atomic and molecular probes such as Scanning Force Microscopy.[4] However, the fabrication of well-defined structures and molecular assemblies from bacterial plasmid DNA as well as their characterization present a much more difficult task. Despite its importance in many biochemical[5] and radiation physics and chemistry [6-44] experiments, plasmid DNA cannot easily be organized into a periodic or quasi-periodic arrangement, particularly, owing to its supercoiled configuration. The problem is particularly acute in experiments with low-penetration-depth (10-100 nm) radiation (e.g., UV photons,[25,34,35,37] soft X-rays [26,29,36] and low energy ions [28,30,33,41,42,43]and electrons[6-24,32,38,39,44]). Irradiations of thin DNA targets with such low range radiation are often performed to investigate the nanoscopic aspects of DNA damage induced by high energy radiation[7,44] xample, in the case of low energy electrons (LEE) experiments, electrons of only 1 to 30 eV energy impinge on a thin DNA film held under ultra high vacuum (UHV). Owing to both short effective range[i] and significant energy loss cross sections of LEEs,[40,44] films have to be very thin (typically 6-10 nm) and deposited on a conducting substrate in order to avoid charging it during electron bombardment. The plasmid DNA films are ordinarily deposited on a metal substrate using the lyophilisation technique before being introduced into UHV.[44] Such

a method produces films which contain clusters of DNA molecules and have irregular thicknesses with ill-defined morphology and surface.[7] Under these conditions, it is still possible to fabricate DNA films which are sufficiently uniform to measure various electron scattering processes and avoid film charging.[44] However, it is difficult to determine the mean free paths and cross sections for electronic excitation, dissociative attachment and induced damage in experiments performed in vacuum.[44] Only a very small amount of degradation species is produced owing to the small film thickness; this condition limits *ex-vacuo* analysis of the degradation products to no other the type of damage than configuration modifications, for which the supercoiled form is needed.[44] The same difficulties arise in experiments with other short-range particles or photons.[25-30,33-37,41-43] Thus, there exists a pressing need to develop methods to fabricate well-ordered plasmid DNA films, which can be characterized on a molecular scale. Such films should be easily redissolved in water for subsequent analysis by chemical methods. We describe in this article a method to fabricate well-characterized dense DNA plasmid layers, created under biogenic conditions and deposited onto an electrical conductor with molecular-level flatness. The method allows one to create well-characterized layers composed of plasmid DNA • diaminopropane cation (Dap^{2+}) complexes designed to erode in water. In the present experiments, the film morphology and surface are analyzed using Atomic Force Microscopy (AFM) and DNA topological isomery by means of gel electrophoresis. The procedure for fabricating layers is described in the experimental section along with a description of the AFM and gel electrophoresis analysis. The results are given and discussed in the next section in relation to present and potential applications. We conclude and summarize our results in the last section of the paper.

Experimental Section

Chemicals and Materials.

Plasmid DNA (pUC21, 3151bp) at initial concentration of 1mg/ml in water for injection (WFI) was obtained from PlasmidFactory GmbH & Co. KG (Germany). Without further purification, a stock solution of this DNA (>95% supercoiled) was prepared by dilution with ultrapure water having a resistivity of 18.2 M Ω.cm. The DNA concentration was determined by measuring the absorbance at 260 nm using the molar extinction coefficient $\varepsilon_{260} = 5.3 \times 10^7$ cm^{-1} M^{-1}.[70] 1,3-Diaminopropane Dihydrochloride (98%) was purchased from Sigma-Aldrich and kept at 4°C. Solutions were freshly prepared before each experiment.

Preparation of DNA Polyelectrolyte • Dap Complexes.

A solution with the appropriate concentration of DNA is mixed with an equal volume of a solution containing protonated 1,3-diaminopropane molecules (Dap^{2+}) to attain the desired $\left[Dap^{2+}\right]/\left[PO_4^-\right]_{DNA}$ molar ratios R $\left(0.1 \le R \le 320\right)$. The excess of positive charges arising from Dap^{2+} cations is defined with respect to R, the ratio of the molar concentrations of those divalent ions to that of anionic phosphate moieties of DNA in the solution. The resulting solutions were mixed and incubated at 25 °C for 15 minutes, then used for the different investigations (UV-spectroscopy, gel electrophoresis and multilayer fabrication). Within our experimental conditions, the pH of the used solutions was ranging from 7.2 to 6.2 in the absence of TRIS/EDTA buffer as measured using a Consort C861 Benchtop Electrochemistry Meter. In the presence of TE buffer, the pH was adjusted to 8.

Multilayer Fabrication and AFM investigation

The deposits were prepared by soft-adsorption (figure 1): A 50-µl droplet of DNA–Dap mixture was deposited onto a freshly cleaved graphite (HOPG, ZYA grade, NT-MDT) surface and incubated during 15 min. Then, the surplus mixture solution was removed using filter paper. After drying in clean air for 3 min, the samples were immediately imaged using atomic force microscopy (AFM). The AFM images were obtained with a Molecular Imaging scanning probe microscope (Agilent now, USA). Silicon nitride tips coated with aluminium (Nanoandmore) at a resonant frequency of 300 kHz in the tapping mode were used to image the topography surface in air, at standard temperature and pressure.

Thickness measurements were performed using the AFM: a small window (1x1µm) was scanned in the contact mode under a loading force appropriate for the tip to remove the deposit without damaging the graphite substrate. Following that step, the snapshots were recorded by scanning a large window (5x5µm) in the tapping mode, which make it easily possible to measure the height of the layers.

Instruments and Methods.

The absorption spectra were recorded using a Varian, Cary 100 Scan, UV-visible spectrophotometer. Quartz reservoirs of 1cm optical path length were used. Hypochromism or hypochromicity [56] refers to a decrease in absorption at a given wavelength, it is defined as:

$$\% \, h_0 = \left[1 - \frac{\varepsilon(\mathrm{DNA} \bullet \mathrm{Dap}^{2+})}{\varepsilon(\mathrm{Pure\ DNA})} \right] \times 100 \qquad (1)$$

Hypochromicity data was computed for the different R values based on the absorption spectra of free DNA and DNA•Dap^{2+} complexes measured at 260 nm. Gel electrophoresis measurements are based on 1% agarose in TAE buffer at 6.7 V.cm−1 for 7 minutes and 5.0 V.cm−1 for 70 minutes. Both the gel and DNA-Dap mixtures were pre-strained with SYBR-

Green 1 (Molecular Probes) (1X for gel and 20X for DNA respectively). Equivalent of one hundred nanograms of DNA was loaded per well. Gels were scanned with Bio-Rad Gel Doc^{TM} XR using blue fluorescence mode at an excitation wavelength of 302 nm. The relative amounts of each form of DNA were obtained from Image analysis by Quantity One software.

Results and Discussion

Preliminary Considerations and Experiments. We first tried to produce films with high coverage using the method described in Figure 1 and by increasing the DNA concentration in the initial solution, this without any buffer or other salts than structural counterions. We found that high coverage could not be achieved following this procedure. Thus, in order to partially screen the repulsive forces between DNA polyions, additional monovalent and divalent cations (Na^+ and Mg^{2+}) have been added to the mother solution and their influence on the topology of the deposited plasmids was followed accurately by AFM.

Even though, the effects of a variation of the ionic strength on plasmid topology in solution are rather well described by thermodynamics, molecular mechanics and molecular dynamics calculations,[47,48] not so much is known about the behavior of partially neutralized polyions adsorbed on a hydrophobic surface. As stated by Fujimoto and Schnurr,[49] confining a supercoiled DNA to a plane greatly restricts its configurational freedom and the number of configurations available (i.e., the configurations of DNA in solution are vastly greater than for surface-confined DNA). However, our results obtained after adsorption on HOPG in the presence of mono and di-valent cations tend to prove that the topology of the plasmids is not greatly modified as compared to an aqueous environment. Briefly, under high ionic strength (NaCl), the plasmids are adsorbed in a fully interwound (plectonemic supercoil) topology, whereas, under low ionic strength they are adsorbed in a quasi-relaxed form (the number of interwindings is low). Adding mono- or divalent cations to the mother solution does not allow

condensation and precipitation of DNA onto HOPG. Only the topology of the plasmids is affected by a variation of the ionic strength, not the number of molecules adsorbed per unit area. As expected, a variation of the pH of the solution no longer increases the covered surface fraction that actually remains low. Thus, we used di-amines in order to condense plasmids and to screen as much as possible the repulsive forces between anionic phosphate groups of the DNA backbone in aqueous solution. Polyamines are indeed known to be involved in the mechanism of DNA folding-unfolding in biological cells[50] as well as stabilization of the negative charges of DNA.[51] Cao and Schuster[52] recently have shown that hydrophobic protection of DNA can be achieved by forming a complex with lipid-like spermine derivatives. Therefore, polyamines complexed with DNA should make it possible to densely pack DNA. We thus expect plasmids to condense more easily onto the surface of hydrophobic HOPG in presence of polyamines than, for example, Poly(β-amino Ester)[53] on planar silicon substrates or Poly(amidoamine)[54] onto muscovite mica. We show in the next subsections that the simple protonated diamine, diamino propane (Dap, also called Z-5), is very efficient to create densely packed DNA plasmid layers designed to erode in aqueous media.

DNA Plasmids Topology in the Presence of Dap^{2+}. Diamino propane is mostly doubly-protonated in water (pK_{a1}= 10.1-10.7, pK_{a2} = 8.3-9.0).[55]

$$\begin{aligned} {}^{+}_{3}HN-(CH_2)_3-NH_2+H_2O &\overset{Ka_1}{\rightleftarrows} {}_{2}HN-(CH_2)_3-NH_2+H_3O^+ \\ {}^{+}_{3}HN-(CH_2)_3-NH_3^+ + H_2O &\overset{Ka_2}{\rightleftarrows} {}^{+}_{3}HN-(CH_2)_3-NH_2+H_3O^+ \end{aligned} \qquad (2)$$

In order to control the DNA conformation, prior to deposition onto HOPG, the UV-absorption spectrum of [DNA • $Dap2^+$] complexes in water was measured at the DNA maximum absorption, i.e. 260 nm. Neither red-, nor blue-shift was observed indicating that the native B form is retained when DNA is complexed with Dap^{2+} ions. Figure 2 shows the variations in

hypochromicity[56] measured for a wide range of R values, where R is the ratio $\left[Dap^{2+}\right]/\left[PO_4^-\right]_{DNA}$. Weak hyperchromicity is observed for small values of R (R = 0.1 and R= 1, see the inset in Figure 2). As for higher R values, hypochromicity rises continually, reaching 12.5% at saturation. For $2 \le R \le 16$, the hypochromicity remains low and reaches 5% at R=16. Hypochromicity is the result of nearest neighbor base pair interactions; it can be due to both intercalation and groove binding.[57] Using molecular dynamics computations, Korolev et al.,[58,59] have shown that Dap^{2+} essentially binds to DNA through O1P, O2P (phosphate moiety) within the minor and major grooves. Binding to the phosphate moiety appears with a clear dominance of coordination to the O1P atom compared to O2P.[58] Furthermore, using the isotopically labeled ammonium ion ($^{15}NH_4^+$) as a probe for high-resolution NMR spectroscopy experiments, Hud and co-workers[60] have shown that there is a preference for the binding of ammonium cations in the minor groove of A-tract sequences in DNA. As shown by Kielkopf and co-workers[61] using high resolution X-Ray Cristallography, the presence of bound ions influences the helical parameters, torsion angles, and hydration of the DNA dimer, which in turn may exhibit hypochromicity. The BI conformation is the nucleotide conformation in the classical B-form of DNA. Multiple conformational states for a same B structure of double stranded DNA (BI-BII equilibria) are nevertheless known[61] to arise. The BII / BI ratio depends on the ligand binding affinity and concentration. Dap binding to DNA may stabilize a certain conformation of the backbone at the expense of entropy. In 95% RH (Relative Humidity), the ratio BII/BI was found to be 0.72 in the presence of Dap^{2+}.[59] Our spectroscopic analyses thus demonstrate that no B→A or B→Z transition occur in the plasmids DNA; only distortions related to BI-BII equilibrium appear in their structure, when R increases and yields high ionic strengths. In the present study, 96.1% of the initial DNA macromolecules are in the supercoiled topological form; the remaining 3.9% adopt the circular (relaxed) form. A large series of aqueous solutions with $0.1 \le C_{DNA} \le 500\,ng/\mu l$ and

$0.1 \leq R \leq 10$ was analysed by means of agarose gel electrophoresis. Data for this series of measurements is graphically displayed in Figure 3. A ratio of R= 0.1 does not notably modify the proportion of supercoiled conformation, while for R reaching greater values (R=1 or R=10), this proportion decreases when C_{DNA} increases, then stabilizes and no longer depend on R. For either R=1 or R=10, the results are very similar. The proportion of supercoiled form decreases and the circular as well as dimer percentages conversely increase and saturate over $C_{DNA} \geq 200$ ng/µl. In the concentration range 50-100 ng/µL the observed variations are particularly drastic. The appearance of dimers as well as the increase in circular conformation highlight DNA damage.[62,63] One single strand break is sufficient to provoke plasmid relaxation (i.e. opening of the plasmid from its supercoiled to the circular form in order to relax torsional stress). Stabilization of the damage rate over $C_{DNA} \geq 200$ ng/µl when $R \geq 1$ is noteworthy, it relate to the saturation of the damaging process in DNA. At least 60% of the supercoiled form remains for whatever are the values of $C_{DNA} > 200$ and $R > 1$. Most importantly, it is clear that in our experiments, DNA damage is undoubtely due to the presence of the Dap^{2+} ions. The same behaviour is observed when using amino propane instead of Dap (not shown here) indicating that the divalent character of Dap^{2+} is not a necessary condition to get the observed damages. The appearance of dimers (i.e. two covalently bound relaxed plasmids) for $C_{DNA} \geq 100$ ng/µl suggests that, within our experimental conditions, two relaxed topoisomers have a significant encounter frequency. To our knowledge, literature data concerning cleavage of DNA by metal-free compounds in the absence of ionising radiations are not as frequent, or even missing. Further investigations are needed to understand the chemical pathways by which DNA cleavage occurs. Important here is the fact that we did use solutions of DNA free of any chemical buffer. We decided therefore to test the possible protecting effect of a buffer, i.e. TRIS-EDTA (TE), against DNA damage. For this reason, we prepared the same solutions as previously mentioned, but in presence of

10 mM TRIS and 1 mM EDTA (pH = 7.8). In Figure 4 we present the % of the observed DNA forms at R=1 when TE buffer is added to the same DNA concentrations as those indicated in Figure 3. The addition of TE has a very stabilising effect. The dimer form no more appears and the % of supercoiled form is now very similar to the reference (see the two lines on the left-handed side of Figure 4); typically a 5% loss of supercoiling is observed with C_{DNA} ranging from 10 to 500 ng.µl^{-1} and R=1.

Making Films with Various Thicknesses. As the major Dap^{2+} binding sites in DNA are the anionic phosphate groups,[57] we guess that Dap^{2+} can act as an ionic binding ligand in order to self-assemble DNA layers onto HOPG. In the absence of TE, it is clear that R=0.1 is the most favorable ratio for depositing undamaged plasmids on the surface. Unfortunately, with this ratio taken at various DNA concentrations, it is impossible to obtain densely-packed layers on the HOPG surface, only sparsely adsorbed plasmids are observed using AFM (Figure 5). With R=1 and C_{DNA} = 100 ng/µl a monolayer (ML) can be produced on a large area typically as large as the contact area of the drop which in our experiments is usually 1 cm^2, whose adhesion/anchoring on the graphite surface prevents DNA release in water. Whatever is the rinsing time, the layer remains entirely confined to the surface. As shown in Figure 6, increasing R makes it possible to self-accumulate thicker layers. Contrary to the first layer, these additional layers are soluble in water.

Characterization of Film Thickness and DNA Release in Water. The height of the formed layers is measured using the profilometry technique: a scratch is made on a small area of the layer with the AFM tip in the contact mode. The localized etching of the surface is then imaged in the tapping mode and a series of height measured along different lines crossing the empty area. This way, the average height of the deposits are measured and reported versus R at a constant DNA concentration. Changing R at constant C_{DNA}, enables layers to be created

starting from a 2 nm insoluble layer up to deposits as thick as several dozen of nanometers. In Figure 7, the mean height of the layers is presented versus R in the case of two different DNA concentrations with or without TE. The plateau-value of the film thickness depends on the DNA concentration, irrespective of the presence or not of TE. Both R and C_{DNA} values dictate the height of the layers and therefore make it possible to control their heights. Acting on these two parameters allows one to construct layers of a well-defined thickness. The total thickness is considered to arise from successive intercalation of diamine molecules bridging the first insoluble monolayer of DNA with the plasmids in its close vicinity (see ISPL in Figure 1). The two plateau values shown in Figure 7 typically correspond to thicknesses of 5 monolayers (ML) (100 ng/µl) and 13 ML (300 ng/µl). Figure 8 shows the evolution of the measured layers thickness versus C_{DNA} with R=1 in the absence of TE. At 100 ng/µl, only the first layer is formed. It is insoluble in water, even if both the incubation time and the number of rinsing (washing) are increased. The mean thickness of that layer was measured to be 2.2 ± 0.5 nm. This value is consistent with the DNA double-strand sectional dimensions (i.e. 2 nm) and demonstrates dense packing and full adherence to HOPG. We guess that such a strong adhesion is due to hydrophobic interactions and site specific anchorage. As 1,3-diaminopropane molecules are in excess compared to the total number of anionic sites in DNA, its full charge is extremely screened and hydrophobic domains cover the DNA grooves that in turn favour hydrophobic interactions with the HOPG surface. Moreover, it is well-known[64] that in the double protonated 1,3-diaminopropane, the all-trans distance between two positively charged ammonium groups is very close to the distance separating two consecutive anionic phosphate groups on the DNA backbone (see SSPB in Figure 1). Molecular dynamic simulations demonstrate that Dap is capable of pronounced narrowing of the minor groove[65] through direct binding to the phosphate groups across the groove (see MGPB in Figure 1). As the Dap^{2+} ammonium moieties are located in close vicinity to the negative DNA phosphate

groups, it is likely that their free aliphatic (i.e. hydrophobic) chains may create short distance interactions with the HOPG surface (SSPB and MGB in Figure 1). Additionally, with their propensity to interact with phosphate moieties, Dap^{2+} molecules exclude water molecules from the close backbone environment and particularly from the minor groove.[61,65] This last behaviour should thus emphasize hydrophobic interactions near to the surface. Moreover, we also verified that when thoroughly rinsed with water, the thick layers are released and the surface gets back to the state of a non-soluble monolayer with a constant thickness of 2.2 ± 0.5 nm. Within any values of C_{DNA} and R, for which thick layers are formed, release in water occurs, except for the first layer that remains anchored to the HOPG surface. Interestingly, specific and local interactions have been shown to appear near to a hydrophobic surface owing to intense local dielectric constant variations at the solid-liquid interface. As shown recently by Lima et al.[66] and Horinek and Netz,[67] a strong ion specific double layer sets in, owing to unequal ion short-range potentials acting between ions and surfaces. Those specific interactions may therefore favour the formation of the first insoluble layer observed in this work. Gel electrophoresis analysis of the DNA plasmids that leached out from the surface into ultra-pure water yield proportions of supercoiled conformation that are close to those measured prior to deposition (Figure 4) in buffered solutions (TE). On the contrary, in the absence of TE buffer, the whole process; mixing DNA with dap, depositing the complex and then leaching it of, is much more damaging. The presence of TE buffer makes it possible for DNA macromolecules to be gently restored in aqueous media with a very acceptable yield of damage. This latter is inversely proportional to the thickness of the layer. We summarize these results in Figure 9. Finally, we note that in relation to potential applications in the field of gene delivery from tissue engineering scaffolds or other techniques related to self-assembly of biomolecules, Dap may pose a problem due to its toxicity. We therefore did test the capabilities of putrescine, a biogenic diamine that contains one more methylene group in its

aliphatic chain, in order to create similar densely packed and releasable layers on HOPG. Intracellular putrescine levels must indeed be significantly increased (> 50 nmol/mg of protein) in order to observe induction of polyamine-mediated gene expression.[68] We found that putrescine used under the same conditions as Dap also makes it possible to accumulate very dense layers of plasmids on HOPG. In Figure 10, we present typical AFM snapshots of layers constructed with R = 2, 4, 8, 16 and C_{DNA} = 20 ng/l. This result may show promise in fields related to surface mediated gene transfer, particularly because the present method could easily be automated and provide well characterized centimetric-sized areas of plasmid layers.

Summary and Conclusion

In aqueous solution, when 1,3-diaminopropane is in excess compared to DNA's phosphate moieties ($R \geq 1$), condensation occurs and precipitation on the hydrophobic surface becomes possible. The first-formed layer is densely-packed and its thickness matches well the DNA double strand cross-sectionnal dimensions. The height of a given deposit is dependant on the concentration of DNA (C_{DNA}) and R. With $R \geq 1$, fixing either C_{DNA} or R, while increasing the remaining parameter gives rise to the formation of layers, whose height reaches saturation. The layer growth and height of the closely and neatly packed plasmid DNA condensates can therefore be controlled and predicted. As shown from AFM images, the plasmids are highly intertwined and linked together when condensed on the graphite surface. We have checked by means of gel electrophoresis analyses that the released plasmids are topologically truly intact. With the exception of BI $\rightarrow$ BII transitions, neither B $\rightarrow$ Z, nor B $\rightarrow$ A transitions are observed. Gel electrophoresis analyses of DNA dissolved in pure water in the presence of various Dap concentrations indicates that a constant amount (~30%) of the supercoiled conformation undergoes relaxation (i.e. transformation into the circular form) and in a lesser

proportion (<10%) dimer formation. In the presence of TE buffer, the proportion of circular DNA drops down to 5 % and the dimer form disappears. By varying the ratio R, layer deposition can successfully be achieved onto the freshly cleaved HOPG surface starting from a thickness of 2.2 ± 0.5 nanometers up to layer depths as large as several dozen of nanometers. This behavior is independent of the presence of TE. When placed in contact with water, the deposits are released and become therefore available for further processes or analyses. In TE buffer, the re-dissolved portion of the supercoiled fraction does not vary so much compared to the fraction in solution before condensation onto HOPG. The amount of supercoiled configuration remaining after re-dissolution is more than sufficient for analysis by electrophoresis. The method described here provides valuable and well characterized DNA-Dap complex deposits which will be extremely useful to study nanoscopic aspects of radiobiology related to DNA damage in experiments based on plasmid relaxation.[6-44] In fact, errors introduced in the determination of fundamental and transportable quantities such as scattering cross sections and attenuation coefficients are highly dependent on variations of target thickness.[15] These fundamental quantities are needed to model the effects of any type of radiation.[69] The present method should make it possible to provide such fundamental parameters in thin DNA films and quantitate the damage to plasmid DNA induced by radiation of low penetrating range (10-100 nm) such as UV photons, soft X-rays, low energy ions and LEEs. More generally, this method may constitute a novel and simple alternative to polyelectrolyte layer fabrication for applications in biological sciences. In these applications, it may be preferable to use a less toxic diamine such as putrescine. As shown in this work, layers of DNA-putrescine complexes can also be assembled onto a HOPG surface.

Acknowledgements:

The authors thank the “Communauté d’Agglomération du Pays de Montbeliard” for their financial support, the French CNRS programme “Interface Physique Chimie Biologie, Soutien à la prise de risque” and the Marie Curie international incoming fellowship program of the European Commission. Thanks are extended to Dr. Elahe Alizadeh for pointing out various experiments with thin DNA films.

References

1. Johnston, A. P. R.; Zelikin, A. N.; Caruso, F. *Adv. Mater.* **2007**, *19*, 3727- 3730.
2. Winfree, E.; Liu, F.; Wenzler, L. A.; Seeman, N. C. *Nature* **1998**, *394*, 539-544.
3. Mirkin, C. A.; Letsinger, R. L.; Mucic, R. C.; Storhoff, J. J. *Nature* **1996**, *382*, 607-609.
4. Bezanilla, M., Manne, S.; Laney, D. E.; Lyubchenko, Y. L.; Hansma, H. G. *Langmuir* **1995**, *11*, 655-659.
5. von Sonntag, C. *Free-radical-induced DNA damage and its repair*, Springer-Verlag: Berlin, 2006.
6. Boudaiffa, B.; Cloutier, P.; Hunting, D.; Huels, M. A.; Sanche, L. *Science* **2000**, *287*, 1658-1662.
7. Sanche, L. *Mass Spectrom. Rev.* **2002**, *21*, 349-369.
8. Boudaïffa, B.; Hunting, D.J.; Cloutier, P.; Huels, M.A.; Sanche, L. *Int. J. Radiat. Biol.* **2000**, *76*, 1209-1221.
9. Boudaïffa, B.; Cloutier, P.; Hunting, D.J.; Huels, M.A.; Sanche, L. *Médecine Science* **2000**, *16*, 1281-1283.
10. Boudaïffa, B.; Cloutier, P.; Hunting, D.J.; Huels, M.A.; Sanche, L. *Radiat. Res*. **2002**, *157*, 227-234.
11. Huels M.A.; Boudaïffa, B.; Cloutier, P.; Hunting, D.J.; Sanche, L. *JACS* **2003**, *125*, 4467-4477.
12. Sanche, L. *Phys. Scr.* **2003**, *68*, C108-C112.
13. Martin, F.; Burrow, P.D.; Cai, Z.; Cloutier, P.; Hunting, D.J.; Sanche, L. *Phys. Rev. Lett*. **2004**, *93*, 068101.

14. Cai, Z.; Cloutier, P.; Sanche, L.; Hunting, D. *Radiat. Res*. **2005***, 164*, 173-179.

15. Panajotovic, R.; Martin, F.; Cloutier, P.; Hunting, D.J.; Sanche, L. *Radiat. Res.* **2006***, 165*, 452-459.

16. Zheng, Y.; Hunting, D.J.; Ayotte, P.; Sanche, L. *Radiat. Res*. **2008**, *169*, 19-27.

17. Zheng, Y.; Hunting, D.J.; Ayotte, P.; Sanche, L. *Phys. Rev. Lett.* **2008,** *100*, 198101.

18. Zheng, Y.; Cloutier, P.; Hunting, D.J.; Sanche, L. *J. Biomed. Nanotechnol*. **2008***, 4*, 469-481.

19. Sanche, L. *Chem. Phys. Lett*. **2009**, *474*, 1-6.

20. Zheng, Y.; Sanche, L. *Radiat. Res.* **2009***, 172*, 114-119.

21. Brun, E.; Cloutier, P.; Sicard-Roselli, C.; Fromm, M.; Sanche, L. *J. Phys. Chem. B* **2009**, *113*, 10008–10013.

22. Dumont, A.; Zheng, Y.; Hunting, D.; Sanche, L. *J. Chem. Phys.* **2010**, *132,* 045102.

23. Zheng, Y.; Sanche, L. *J. Chem. Phys.* **2010**, 133, 155102.

24. Alizadeh, E.; Cloutier, P.; Hunting, D.; Sanche, L. *J. Phys. Chem. B* **2011**, *115*, 4523-4531.

25. Folkard, M.; Prise, K.M. *Acta Physica Polonica*, **2006**, *109*, 265-271.

26. Hieda, K.; Hirono, T.; Azami, A.; Suzuji, M.; Furusawa, Y.; Maezawa, H.; Usami, N.; Yikoya, A.; Kobayashi, K. *Int. J. Radiat. Biol*. **1996**, *70*, 437-445.

27. Ptasińska, S.; Bahnev, B.; Stypczynska, A.; Bowden, M.; Mason, N.J.; Braithwaite, N.St.J. *Phys. Chem. Chem. Phys*. **2010**, *12*, 7779-7781.

28. Hunniford, C.A.; McCullough, R.W.; Davies, R.J.H.; Timson, D. *J. Biochem. Soc. Trans*. **2009**, *37*, 893-896.

29. Folkard, M.; Prise, K.M.; Brocklehurst, B.; Michael, B.D. *J. Phys. B: At. Mol. Opt. Phys*. **1999**, *32*, 2753-2761.

30. Sellami, L.; Lacombe, S.; Hunting, D.; Wagner, R.J.; Huels, M.A. *Rev. Sci. Instrum*. **2007**, *78*, 085111.

31. Jiang, Y.; Ke, C.; Mieczkowskiy, P.A.; Marszalek, P.E. *Biophys. J.* **2007**, *93*, 1758-1767.

32. Chen, Y.; Aleksandrov, A.; Orlando, T.M. *Int. J. Mass Spectrom*. **2008**, *277*, 314-320.

33. Huels, M.A.; Imhoff, M.; Zongwu, D. *Int. J. Mass Spectrom.* **2005**, *245*, 68-77.

34. Folkard, M.; Prise, K.M.; Vojnovic, B.; Brocklehurst, B.; Michael, B.D. *Int.J. radiat. Biol.* **2000**, *76*, 763-771.

35. Michael, B.D.; Prise, K.M.; Folkard, M.; Vojnovic, B.; Brokclehurst, B.; Munro, I.H.; Hopkirk, A. *Int.J. Radiat. Biol.* **1994**, *66*, 569-572.

36. Yokoya, A.; Cunniffe, S.M.T.; Watanabe, R., Kobayashi, K., O'Neill, P. *Radiat. Res*. **2009**, *172*, 296-305.

37. Hieda, K.; Suzuki, K.; Hirono, T.; Suzuki, M.; Furusawa, Y. *J. Radiat. Res.* (Tokyo) **1994**, *35*, 104-111.

38. Grieves, G.A.; McLain, J.L.; Orlando, T.M. in *Charged Particles and Photons Interactions with Matter*, Hatano, Y.; Katsumura, Y., Mozumder, A.M. (eds) CRC Press, Boca Raton, USA, **2011**.

39. Orlando, T.M.; Oh, D.; Chen, Y.; Aleksandrov, A.B. *J. Chem. Phys*. **2008**, *128*, 195102.

40. Bass, A. D.; Sanche, L. Radiat. Environ. Biophys. **1998***, 37*, 243-257.

41. Sarapirom, S.; Sangwijit, K.; Anuntalabhochai, S.; Yu, L.D. *Surf. Coat. Technol.* **2010**, *204*, 2960-2965.

42. Lacombe, S.; Le Sech, C.; Esaulov, V.A. *Phys. Med. Biol*. **2004**, *49*, N65-N73.

43. Hunniford, C.A.; Timson, D.J.; Davies, R.J.H., McCullough, R.W. *J. Phys. Conf. Series* **2007**, *58*, 355-358.

44. L. Sanche, "Low-Energy Electron Interaction with DNA: Bond Dissociation and Formation of Transient Anions, Radicals and Radical Anions" in *Wiley Series on Reactive Intermediates in Chemistry and Biology entitled Radicals in Nucleic Acids*, M. Greenberg, ed., John Wiley & Sons (2009).

45. Meesungnoen, J.; Jay-Gerin, J.-P.; Filali-Mouhim, A.; Mankhetkorn, S. *Radiat. Res.* **2002,** *158*, 657-660.

46. Śmiałek, M.A.; Balog, R.; Jones, N.C.; Field, D. ; Mason, N. *J. Eur. Phys. J. D*. **2010**, *60*, 31-36.

47. Fenley, M. O.; Olson, W. K.; Manning, G. S. *Macromolecules* **2000**, *33*, 1899-1903.

48. Bai, Y.; Greenfeld, M.; Travers, K. J.; Chu, V. B.; Lipfert, J.; Doniach, S.; Herschlag D. *J. Am. Chem. Soc.* **2007**, *129*, 14981-14988.

49. Fujimoto, B. S.; Schurr, J. M. *Biophys. J.* **2002,** *82,* 944–962.

50. Larqué, E.; Sabater-Molina, M.; Zamora S. *Nutrition* **2007,** *23*, 87–95.

51. Koculi, E.; Thirumalai, D.; Woodson, S. A. *J. Mol. Biol.* **2006**, *359*, 446–454.

52. Cao, H.; Schuster, G. B. *Bioconjugate Chem.* **2005**, *16*, 820−826.

53. Zhang, J.; Montaez, S. I.; Jewell, C. M.; Lynn, D. M. *Langmuir* **2007**, *23*, 11139-11146.

54. Su, C.-J.; Liu, Y.-C.; Chen, H.-L.; Li, Y.-C.; Lin, H.-K.; Liu, W.-L.; Hsu, C.-S. (58) *Langmuir* **2007**, *23*, 975-978.

55. Bryantsev, V. S.; Diallo, M. S.; Goddard, W. A. *J. Phys. Chem. A* **2007**, *111*, 4422-4430.

56. Bloomfield, V. A.; Crothers, D. M.; Tinoco, I. Jr. In *Nucleic Acids: Structures, Properties, and Functions*. University Science Books: Sausalito, CA, **2000**.

57. Modukuru, N. K.; Snow, K. J.; Perrin, B. S. Jr.; Bhambhani, A.; Duff, M.; Kumar C.V. *J. Photochem. Photobiol. A* **2006**, *177*, 43–54.

58. Korolev, N.; Lyubartsev, A. P.; Laaksonen, A.; Nordenskiöld, L. *Biopolymers* **2004**, *73*, 542–555.

59. Korolev, N.; Lyubartsev, A. P.; Laaksonen, A.; Nordenskiöld, L. *Nucleic Acids Res*. **2003**, *31*, 5971-5981.

60. Hud, N. V.; Sklenář, V.; Feigon, J. *J. Mol. Biol.* **1999,** *286*, 651–660

61. Kielkopf, C. L.; Ding, S.; Kuhn, P.; Rees, D. C. *J. Mol. Biol*. **2000**, *296*, 787–801.

62. Vinograd, J.; Lebowitz, J.; Radloff, R.; Watson, R.; Laipis, P. *Proc. Natl Acad. Sc.i USA* **1965,** *53*, 1104–1111.

63. Boichot, S.; Fromm, M.; Cunniffe, S.; O'Neill, P.; Labrune, J.C.; Chambaudet, A.; (68) Delain, E.; Le Cam, E. *Radiat. Prot. Dosim*. **2002**, *99*, 143-146.

64. Narayana, N.; Shamala, N.; Ganesh, K. N.; Viswamitra, M. A. *Biochemistry* **2006,** *45*, 1200-1211.

65. Korolev, N.; Lyubartsev, A. P.; Laaksonen, A.; Nordenskiöld, L. *Eur. Biophys. J*. **2004** *33*, 671–682.

66. Lima, E. R. A.; Horinek, D.; Netz, R. R.; Biscaia, E. C.; Tavares, F. W.; Kunz, W.; Boström, M. *Phys. Chem. B* **2008**, *112*, 1580–1585.

67. Horinek, D.; Netz, R.R. *Phys. Rev. Let.* **2007**, *99*, 226104.

68. Wang J.-Y., Casero R. A., In *Polyamine Cell Signalling: Physiology, Pharmacology, and Cancer Research*. Humana Press, **2006,** 29-37.

69. Nikjoo, H.; Emfietzoglou, D.; Watanabe, R.; Uehara, S. *Radiat. Phys. Chem*. **2008**, *77*, 1270-1279.

70. Manchester, K. L. *Biotechniques* **1996**, *20*, 968.

Figure Captions

Figure 1: Left is a schematic illustration of the preparation of densely packed [DNA Plasmid • Dap^{2+}] complex layers using a method based on soft-adsorption. The right-handed part of the Figure shows the specific sites where the Dap^{2+} cations interact with the DNA phosphate moieties. SSPB stands for Single Strand Phosphate Binding, MGPB stands for Minor Groove Phosphate Binding and ISPL stands for Inter Strand Phosphate Linking. For a better description of the sites involved in electrostatic interactions, on the left-handed "stick" DNA model, only phosphate atoms (yellow) are shown as "balls". An AFM snapshot, where single plasmids are resolved, illustrates the typical feature of the first layer in which DNA plasmids appear under the form of fully intertwined rods (C_{DNA}=10ng/µl and R= 3).

Figure 2: Hypochromicity measured @ 260 nm for R ranging from 0.1 to 320 in ultra-pure water. ε(ref) corresponds to the maximum absorption of pure DNA plasmids in ultra-pure water. [56] The DNA concentration in these experiments is 50 ng/µl. The inset shows the low hyperchromic effect measured when R≤2. The dashed lines are drawn to guide the eye.

Figure 3: % of supercoiled (SC), Circular (C) and Dimer (D) conformations for various DNA concentrations and ratios R. The dotted and dashed lines represent, respectively, the initial supercoiled and circular forms present in the mother solution. The error bars correspond to the highest standard deviation observed (2.5%) over all average values calculated for each point with 3 different series of measurements. The solid lines are drawn to guide the eye.

Figure 4: % of supercoiled (SC) and Circular (C) conformations for various DNA concentrations at a ratio R=1 in the presence of 10 mM TRIS and 1 mM EDTA (pH=7.8). Two measurements were performed by gel electrophoresis for each DNA concentration.

Figure 5: AFM (5x5 µm) tapping mode image of plasmid DNA – Dap^{2+} complexes formed with R=0.1 and C_{DNA} = 200 ng/µl. Plasmids appear fully intertwined and are mostly isolated from each other. Dimers are exceptionally present (arrows) which confirm that the encounter frequency of the plasmids in solution is notable. The dashed lines indicate a region where plasmids did specifically adsorb parallel to an atomic-scale step on the HOPG surface. The maximum height measured for the deposited plasmids reaches 3.5 nm, therefore we can consider that with a DNA cross-sectional diameter of 2 nm, the plasmids are not fully adsorbed on the surface, but only partially anchored.

Figure 6: AFM (5x5 µm) tapping mode images of layers composed of [plasmid DNA • Dap^{2+}] complexes with R=1, 2, 8 and 32 and C_{DNA} = 20 ng/µl. On the first AFM snapshot (R=1), the inset shows a 6-fold magnification of an area of the deposit where a hole exists. This inset shows clearly the pristine HOPG surface present under the first layer, which is particularly dense. For R=1, some plasmids start to form a layer and exhibit a fibrous shape, indicating a fully intertwined conformation due to a high degree of complexation. It is clear also that several plasmids are linked together in order to form fibres. Varying R from 2 to 8 then to 32, a progression toward the formation of a second layer covering the first one is clearly evidenced.

Figure 7: Average thickness of the layers as a function of the ratio R at two different DNA concentrations with and without TE as measured by AFM. Error bars represent the standard deviations of 10 measurements. The dashed lines are drawn to guide the eye.

Figure 8: Evolution of the layer's mean thickness for various DNA concentrations in the special case where Dap^{2+} and DNA phosphate moieties concentrations are equi-molar, in the absence of TE. Error bars represent the standard deviations of ten different height measurements. The height of the monolayer was measured = 2.2 ± 0.5 nm. The plateau corresponds typically to a 5-layer self assembly. The thin dashed line is drawn to guide the eye.

Figure 9: Summary of the various average percentages of supercoiled DNA after the different steps necessary to release the complexes in water. The protecting effect of TE, which allows restoring plasmids in water with minimal damage, is clearly evidenced. The average values correspond to ten measurements and are presented together with their statistical standard deviation. The thicknesses of the layers are expressed in terms of monolayers (ML); one ML typically corresponds to 2.2 ± 0.5 nm. Thin layers are more fragile than thicker ones.

Figure 10: 4x4 µm snapshots of layers formed on freshly cleaved HOPG with putrescine as a electrostatic linker, R = 2, 4, 8, 16 and C_{DNA} = 20 ng/µl. The white segment on the R=8 image corresponds to 1 µm.

Figures

Figure 1

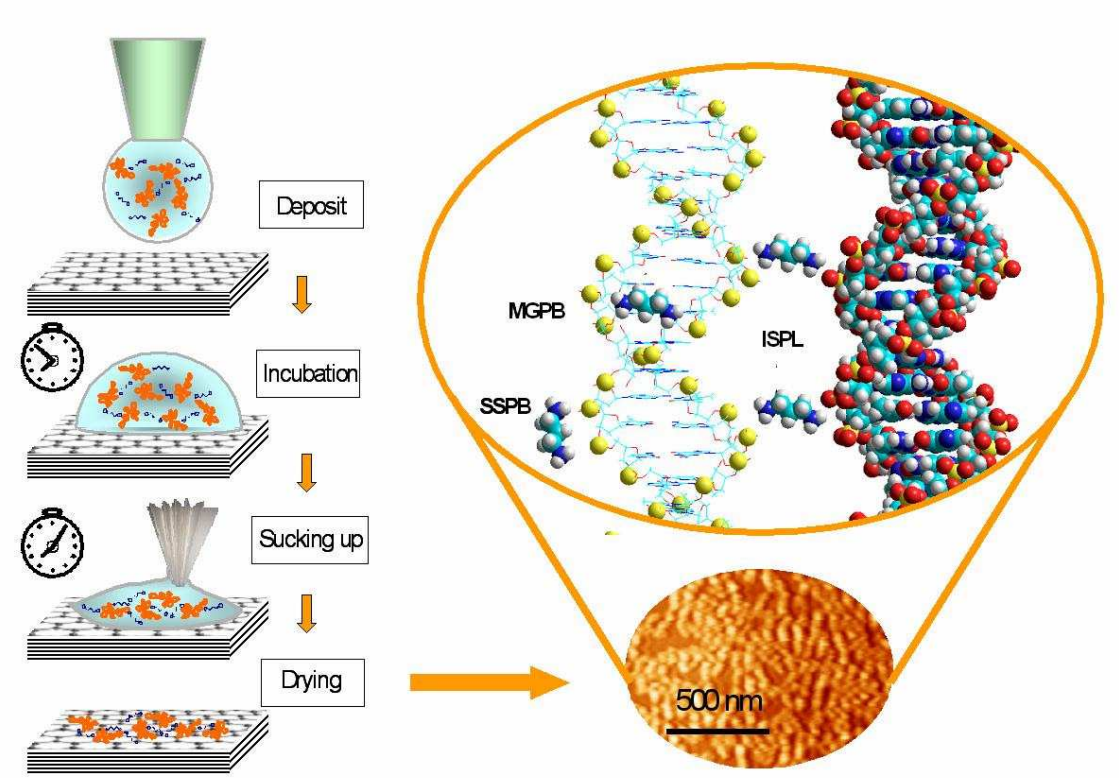

Figure 2

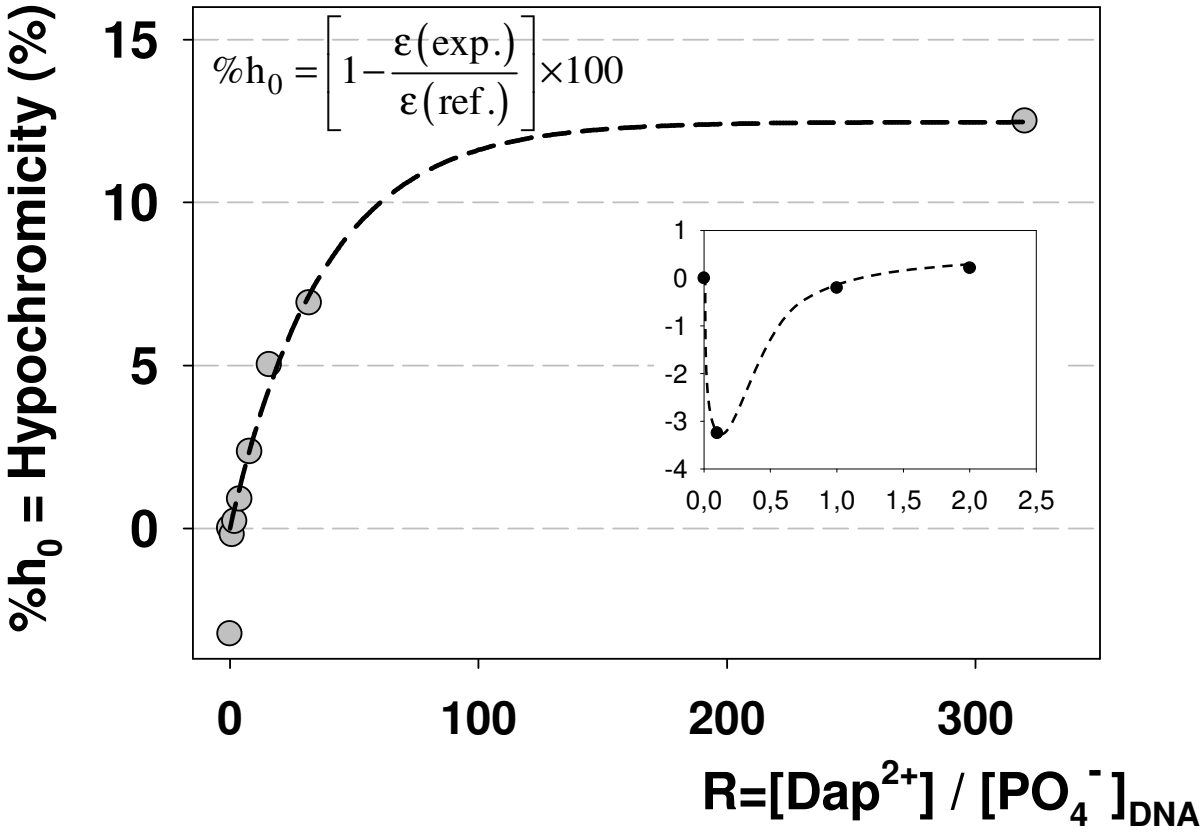
$\%h_0 = \left[1 - \frac{\varepsilon(\text{exp.})}{\varepsilon(\text{ref.})}\right] \times 100$
%h0 = Hypochromicity (%)
15
10
5
0
0
100
200
300
R=[Dap2+] / [PO4-]DNA
1
0
-1
-2
-3
-4
0,0
0,5
1,0
1,5
2,0
2,5

Figure 3

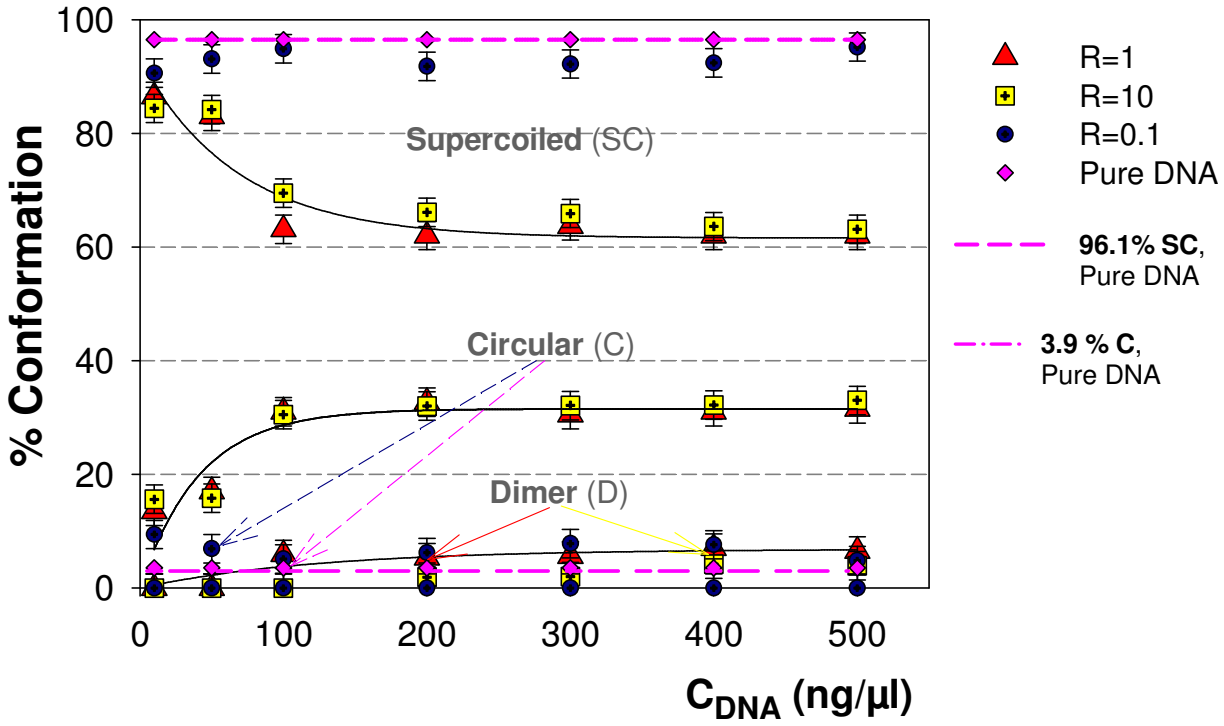
100
80
60
40
20
0
% Conformation
0
100
200
300
400
500
C_DNA (ng/µl)
Supercoiled (SC)
Circular (C)
Dimer (D)
R=1
R=10
R=0.1
Pure DNA
96.1% SC, Pure DNA
3.9 % C, Pure DNA

Figure 4

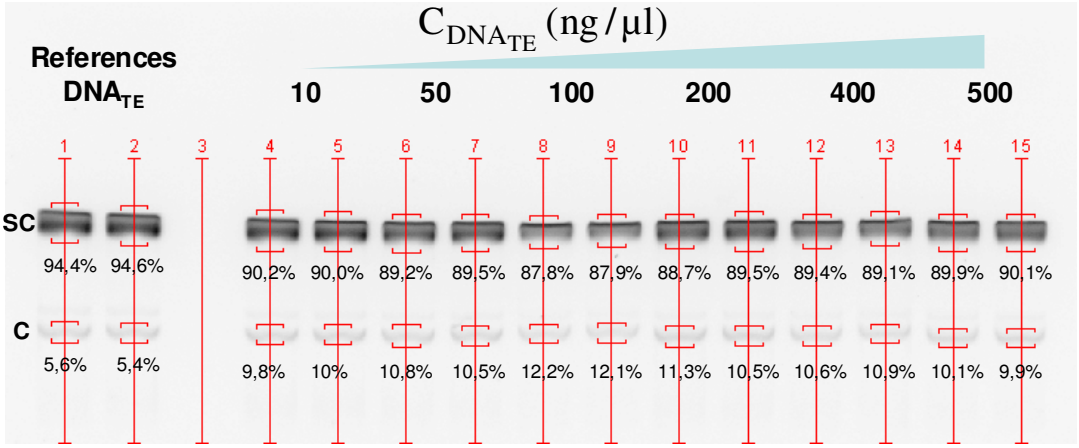
$C_{DNA_{TE}}$ (ng/µl)
References DNA$_{TE}$
10
50
100
200
400
500
1 2 3 4 5 6 7 8 9 10 11 12 13 14 15
SC
C
94,4% 94,6%
90,2% 90,0% 89,2% 89,5% 87,8% 87,9% 88,7% 89,5% 89,4% 89,1% 89,9% 90,1%
5,6% 5,4%
9,8% 10% 10,8% 10,5% 12,2% 12,1% 11,3% 10,5% 10,6% 10,9% 10,1% 9,9%

Figure 5

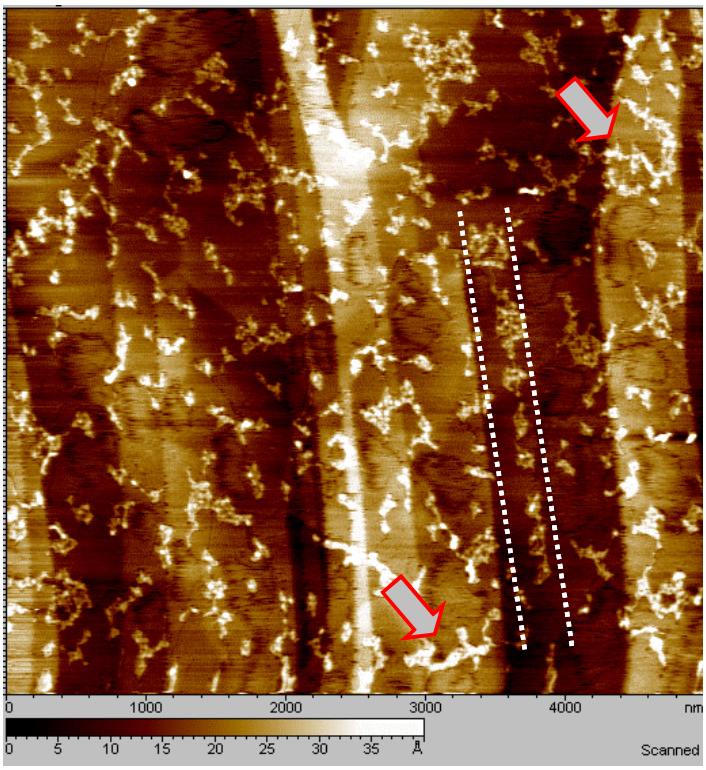

Figure 6

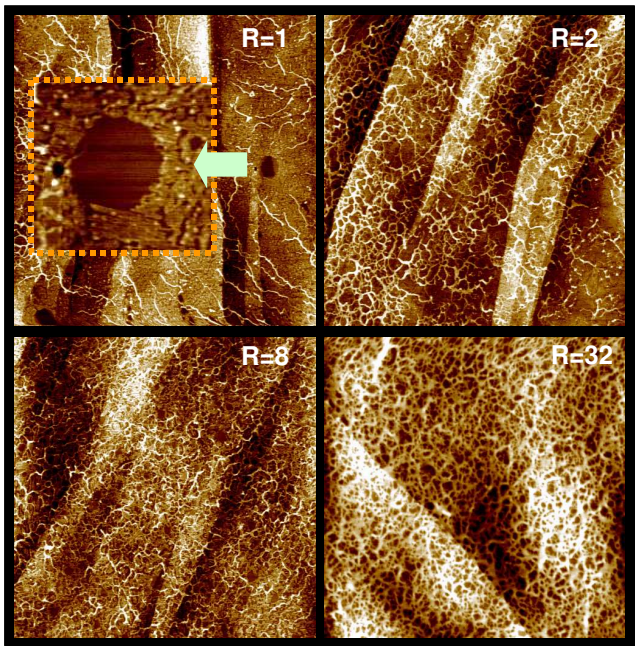

Figure 7

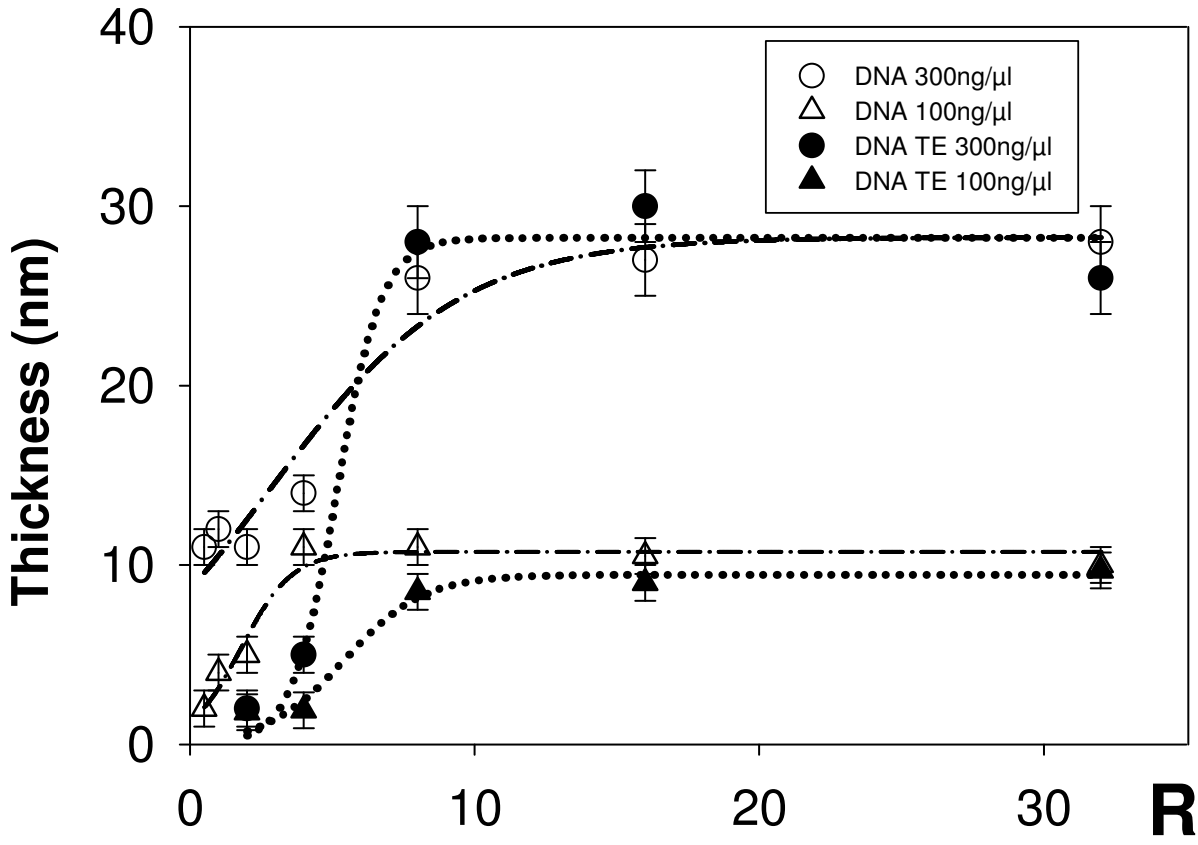
Thickness (nm)
40
30
20
10
0
0
10
20
30
R
DNA 300ng/µl
DNA 100ng/µl
DNA TE 300ng/µl
DNA TE 100ng/µl

Figure 8

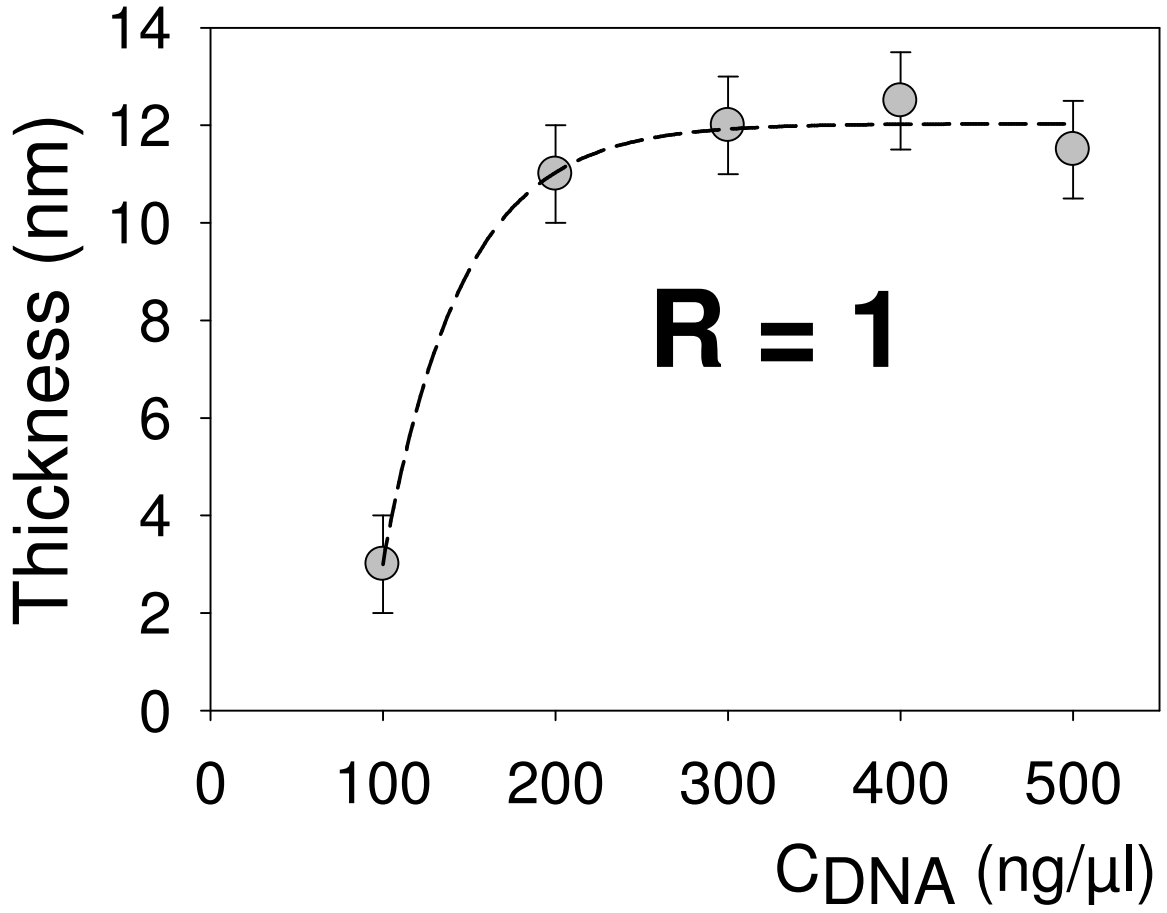

Figure 9

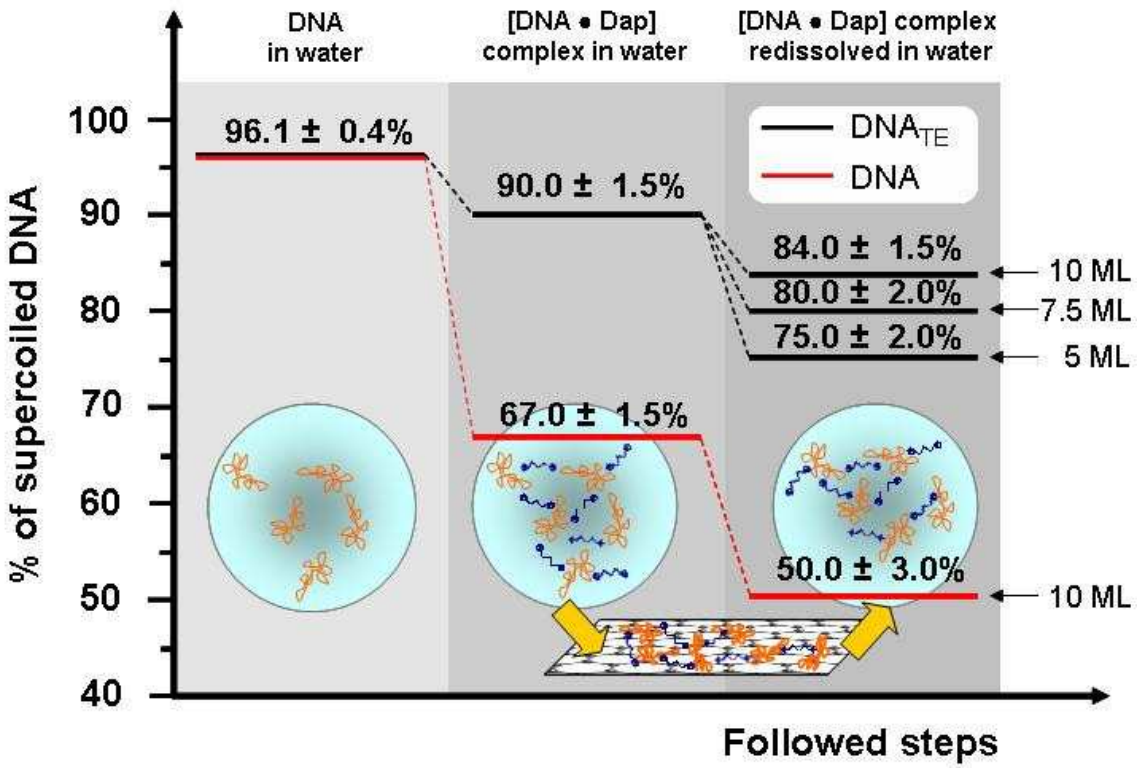
DNA
in water
[DNA • Dap]
complex in water
[DNA • Dap] complex
redissolved in water
DNA$_{TE}$
DNA
96.1 ± 0.4%
90.0 ± 1.5%
84.0 ± 1.5%
80.0 ± 2.0%
75.0 ± 2.0%
67.0 ± 1.5%
50.0 ± 3.0%
10 ML
7.5 ML
5 ML
10 ML
% of supercoiled DNA
100
90
80
70
60
50
40
Followed steps

Figure 10

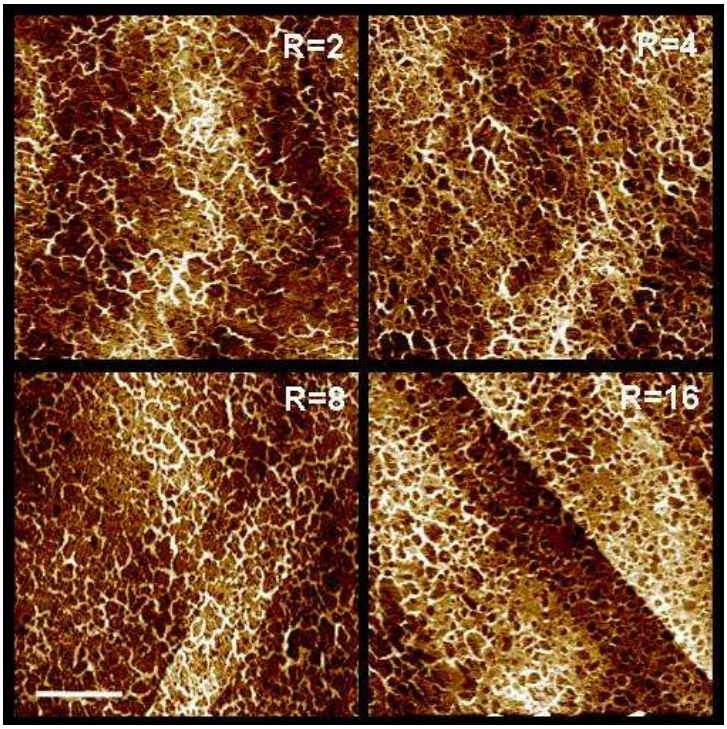

TOC GRAPHIC

(Figure 9)